Supporting Information

Yeh et al. 10.1073/pnas.1701390115

SI Text

System Hamiltonian for Vibronic Aggregates. For each chromophore j, the electronic ground ($|0\rangle$) and first excited ($|j\rangle$) states are coupled to a single intramolecular vibrational mode (described as a harmonic oscillator) with frequency ω_j. The single chromophore Hamiltonian then reads as:

$$\begin{aligned}\hat{H}_j = &\left[\frac{\hat{p}_j^2}{2m_j} + \frac{m_j}{2}\omega_j^2\hat{x}_j^2\right]|0\rangle\langle 0| \\ &+ \left[E_j + \frac{\hat{p}_j^2}{2m_j} + \frac{m_j}{2}\omega_j^2(\hat{x}_j - d_j)^2\right]|j\rangle\langle j| \ .\end{aligned} \quad [S1]$$

Within the above, $\hat{x}_j$, $\hat{p}_j$, m_j, and d_j are, respectively, the coordinate, momentum, mass, and coordinate displacement in the excited state. After introducing the bosonic creation ($\hat{a}_j^\dagger = \hat{x}_j\sqrt{m_j\omega_j/2\hbar} - i\hat{p}_j\sqrt{1/2\hbar m_j\omega_j}$) and annihilation ($\hat{a}_j = \hat{x}_j\sqrt{m_j\omega_j/2\hbar} + i\hat{p}_j\sqrt{1/2\hbar m_j\omega_j}$) operators and subsequently substituting them into Eq. S1, we thus obtain:

$$\begin{aligned}\hat{H}_j = &\hbar\omega_j(\hat{a}_j^\dagger\hat{a}_j + \frac{1}{2}) \\ &+ \left[E_j + \hbar\omega_j\left(S_j - \sqrt{S_j}\left(\hat{a}_j^\dagger + \hat{a}_j\right)\right)\right]\hat{F}_j^\dagger\hat{F}_j \ ,\end{aligned} \quad [S2]$$

where $S_j = m_j\omega_j d_j^2/2\hbar$ is the dimensionless Huang-Rhys factor. $\hat{F}_j^\dagger$ and $\hat{F}_j$ are the electronic excitation and deexcitation operators, defined by $\hat{F}_j^\dagger|0\rangle = |j\rangle$ and $\hat{F}_j|j\rangle = |0\rangle$. Under the local vibronic basis, the vibronic states associate with the electronic ground state and the first excited state can be represented, respectively, by:

$$|g_j^{i_j}\rangle = \frac{(\hat{a}_j^\dagger)^{i_j}}{\sqrt{i_j!}}|g_0\rangle \ , \text{ and } |e_j^{i_j}\rangle = \hat{F}_j^\dagger\frac{(\hat{a}_j^\dagger)^{i_j}}{\sqrt{i_j!}}|g_0\rangle \ . \quad [S3]$$

Where within the above, i_j is the vibrational quanta of the j^{th} chromophore, and $|g_0\rangle$ is the zero-exciton–vibrational ground state (the vacuum state).

After including the electronic coupling, J_{jl}, between chromophores j and l, the system Hamiltonian of vibronic aggregates is expressed as:

$$\begin{aligned}\hat{H}_{\rm V} = &\sum_j E_j\hat{F}_j^\dagger\hat{F}_j + \sum_{j\neq l}J_{jl}\hat{F}_j^\dagger\hat{F}_l + \sum_j\hbar\omega_j\left(\hat{a}_j^\dagger\hat{a}_j + \frac{1}{2}\right) \\ &+ \sum_j\hbar\omega_j\left[S_j - \sqrt{S_j}\left(\hat{a}_j^\dagger + \hat{a}_j\right)\right]\hat{F}_j^\dagger\hat{F}_j \ .\end{aligned} \quad [S4]$$

When simulating the 2DES via the third order nonlinear response function (Eq. S24), one must include the electronic ground states ($|g^{(i_1,i_2,\cdots,i_N)}\rangle \equiv \prod_j|g_j^{i_j}\rangle$), singly excited electronic states ($|e_m^{(i_1,i_2,\cdots,i_N)}\rangle \equiv |e_m^{i_m}\prod_{j\neq m}g_j^{i_j}\rangle$), and doubly excited electronic states ($|f_{uv}^{(i_1,i_2,\cdots,i_N)}\rangle \equiv |e_u^{i_u}e_v^{i_v}\prod_{j\neq u,v}g_j^{i_j}\rangle$). For convenience, an N-component vector, $\mathbf{i} = (i_1, i_2, \cdots, i_N)$, is introduced and the above basis states now read as $|g^{\mathbf{i}}\rangle$,$|e_m^{\mathbf{i}}\rangle$, and $|f_{uv}^{\mathbf{i}}\rangle$ ($u < v$). The one- and two-exciton eigenstates of $\hat{H}_{\rm V}$ are $|e_p\rangle = \sum_m\sum_{\mathbf{i}}\psi_{p,\mathbf{i}}^m|e_m^{\mathbf{i}}\rangle$ and $|f_r\rangle = \sum_{u<v}\sum_{\mathbf{i}}\Psi_{r,\mathbf{i}}^{uv}|f_{uv}^{\mathbf{i}}\rangle$, respectively. The electronic contribution of a one-exciton eigenstate, p, is defined as its total overlap with pure electronic states:

$$\chi_{p,el} = \left(\psi_{p,\{0,0\}}^1\right)^2 + \left(\psi_{p,\{0,0\}}^2\right)^2 \ . \quad [S5]$$

The final system Hamiltonian, $\hat{H}_{\rm S}$, used in the calculations are $\hat{H}_{\rm E}$ for ED and $\hat{H}_{\rm V}$ for VD.

Total Hamiltonian. All the other vibrational modes (from protein and/or solvent fluctuations) that couple to each chromophore are modeled as an independent phonon bath composed of harmonic oscillators, described by:

$$\hat{H}_{\rm B} = \sum_{j=1}^N\sum_\xi\frac{\hat{p}_{j\xi}^2}{2m_{j\xi}} + \frac{1}{2}m_{j\xi}\omega_{j\xi}^2\hat{x}_{j\xi}^2 \ , \quad [S6]$$

where $m_{j\xi}$, $\omega_{j\xi}$, $\hat{x}_{j\xi}$, $\hat{p}_{j\xi}$ are the mass, the frequency, the position and the momentum operator of the ξ^{th} bath oscillator associated with the j^{th} chromophore, respectively. For the system-bath interaction, we assume the system is affected by the phonon bath through electronic energy fluctuations and vibrational relaxation, and hence the Hamiltonian has the form:

$$\begin{aligned}\hat{H}_{\rm SB} &= \eta_{\rm E}\sum_{j=1}^N\sum_\xi c_{j\xi}\hat{x}_{j\xi}\hat{F}_j^\dagger\hat{F}_j + \frac{\eta_{\rm V}}{\sqrt{2}}\sum_{j=1}^N\sum_\xi c_{j\xi}\hat{x}_{j\xi}(\hat{a}_j^\dagger + \hat{a}_j) \\ &= \sum_{j=1}^N\hat{V}_j\sum_\xi c_{j\xi}\hat{x}_{j\xi} = \sum_{j=1}^N\hat{V}_j\hat{B}_j \ .\end{aligned} \quad [S7]$$

In the above equation, $\hat{B}_j = \sum_\xi c_{j\xi}\hat{x}_{j\xi}$ is defined as the collective bath operator and $\hat{V}_j \equiv \eta_{\rm E}\hat{F}_j^\dagger\hat{F}_j + \eta_{\rm V}(\hat{a}_j^\dagger + \hat{a}_j)/\sqrt{2}$ is a system operator, where the first and the second terms represent the bath-induced electronic energy fluctuations and vibrational relaxation, respectively. The reorganization energy that counteracts the shifted equilibrium position of bath oscillators thus has the form of $H_{\rm reorg} = \sum_{j=1}^N\sum_\xi c_{j\xi}^2\hat{V}_j^2/2m_{j\xi}\omega_{j\xi}^2$. One then obtains an effective system Hamiltonian that includes the above counter term as $\hat{H}_{\rm eff} = \hat{H}_{\rm S} + \hat{H}_{\rm reorg}$, and the total Hamiltonian becomes $\hat{H}_{\rm tot} = \hat{H}_{\rm eff} + \hat{H}_{\rm B} + \hat{H}_{\rm SB}$.

System Hamiltonian for Linear and 2D Spectra Calculation. For simulating the 2D electronic spectra (2DES), one needs to include the electronic ground state, singly excited states, and doubly excited states of the molecular aggregates. We can then rearrange the Hamiltonian into a block diagonal matrix by ascending number of excitons. In the ED case it has the form:

$$\hat{H}_{\rm S,ED}^{\rm 2D} = \begin{pmatrix} H_{\rm g} & 0 & 0 \\ 0 & H_{\rm 1ex} & 0 \\ 0 & 0 & H_{\rm 2ex}\end{pmatrix} \ , \quad [S8]$$

with $H_{\rm g} = E_0|0\rangle\langle 0| = 0$, the single exciton manifold is

$$H_{\rm 1ex} = \sum_j E_j|j\rangle\langle j| + \sum_{j\neq l}J_{jl}|j\rangle\langle l| \ , \quad [S9]$$

and the elements in the biexciton manifold read:

$$\begin{aligned}\langle jl|\, H_{2\mathrm{ex}}\, |j'l'\rangle &= \delta_{jj'}\delta_{ll'}(E_j+E_l)+\delta_{jj'}(1-\delta_{ll'})J_{ll'}\\ &+\delta_{jl'}(1-\delta_{lj'})J_{lj'}+\delta_{lj'}(1-\delta_{jl'})J_{jl'}\\ &+\delta_{ll'}(1-\delta_{jj'})J_{jj'}\ .\end{aligned} \tag{S10}$$

The same block diagonal structure also applies to the vibronic case. However, in this case there are vibrational states associated to the electronic ground state, and the elements in the electronic ground state Hamiltonian can be written as:

$$H^{\mathrm{gg}}_{\mathbf{i},\mathbf{i}'} \equiv \langle g^{\mathbf{i}}|\, \hat{H}_{\mathrm{V}}\, |g^{\mathbf{i}'}\rangle = \left[\sum_j \hbar\omega_j\left(i_j+\frac{1}{2}\right)\right]\delta_{\mathbf{i}\mathbf{i}'}\ , \tag{S11}$$

where $\delta_{\mathbf{i}\mathbf{i}'}\equiv\prod_l \delta_{i_l i'_l}$. The singly excited states Hamiltonian is then given by:

$$\begin{aligned}H^{(\mathrm{e}_m\mathrm{e}_{\tilde{m}})}_{\mathbf{i}\mathbf{i}'} &\equiv \langle e^{\mathbf{i}}_m|\, \hat{H}_{\mathrm{V}}\, |e^{\mathbf{i}'}_{\tilde{m}}\rangle = \delta_{\mathbf{i}\mathbf{i}'}\,(1-\delta_{\mathrm{m}\tilde{\mathrm{m}}})\,J_{\mathrm{m}\tilde{\mathrm{m}}}\\ &+\delta_{\mathbf{i}\mathbf{i}'}\delta_{\mathrm{m}\tilde{\mathrm{m}}}\left[E_m+\hbar\omega_m S_m+\sum_j \hbar\omega_j\left(i'_j+\frac{1}{2}\right)\right]\\ &-\hbar\omega_m\sqrt{S_m}\delta_{\mathrm{m}\tilde{\mathrm{m}}}\left\langle i_m, i'_m\right\rangle\prod_{l,l\neq m}\delta_{i_l i'_l}\ ,\end{aligned} \tag{S12}$$

where the vibrational wavefunction integral is defined as:

$$\begin{aligned}\left\langle i_m, i'_m\right\rangle &\equiv \langle g^{i_m}_m|\,\left(\hat{a}^\dagger_m+\hat{a}_m\right)|g^{i'_m}_m\rangle\\ &=\sqrt{i_m}\delta_{i_m-1,i'_m}+\sqrt{i'_m}\delta_{i_m+1,i'_m}\ .\end{aligned} \tag{S13}$$

Similarly, the Hamiltonian of doubly excited states reads:

$$\begin{aligned}H^{(\mathrm{f}_u\mathrm{f}_{u'}\mathrm{f}_{v'})}_{\mathbf{i}\mathbf{i}'} &= \delta_{\mathbf{i}\mathbf{i}'}\left[E_u+E_v+\sum_j\hbar\omega_j\left(i_j+\frac{1}{2}\right)\right]\delta_{uu'}\delta_{vv'}\\ &+\delta_{\mathbf{i}\mathbf{i}'}\left[J_{uu'}\left(1-\delta_{uu'}\right)\delta_{vv'}+J_{vu'}\delta_{uv'}\right.\\ &\left.+J_{uv'}\delta_{vu'}+J_{vv'}\left(1-\delta_{vv'}\right)\delta_{uu'}\right]\\ &-\hbar\omega_u\sqrt{S_u}\delta_{uu'}\delta_{vv'}\left\langle i_u, i'_u\right\rangle\prod_{l,l\neq u}\delta_{i_l i'_l}\\ &-\hbar\omega_v\sqrt{S_v}\delta_{uu'}\delta_{vv'}\left\langle i_v, i'_v\right\rangle\prod_{l,l\neq v}\delta_{i_l i'_l}\\ &+\delta_{\mathbf{i}\mathbf{i}'}\left(\hbar\omega_u S_u+\hbar\omega_v S_v\right)\delta_{uu'}\delta_{vv'}\ ,\end{aligned} \tag{S14}$$

and therefore the resulting Hamiltonian for simulating 2D spectra of VD is:

$$\hat{H}^{\mathrm{2D}}_{\mathrm{S,VD}} = \begin{pmatrix} H^{\mathrm{gg}} & 0 & 0\\ 0 & H^{\mathrm{ee}} & 0\\ 0 & 0 & H^{\mathrm{ff}}\end{pmatrix}\ . \tag{S15}$$

When simulating linear spectra, only the electronic ground state and the first excited states are included, so the Hamiltonian for ED and VD become:

$$\hat{H}^{\mathrm{1D}}_{\mathrm{S,ED}} = \begin{pmatrix} H_{\mathrm{g}} & 0\\ 0 & H_{1\mathrm{ex}}\end{pmatrix}\ , \tag{S16}$$

and

$$\hat{H}^{\mathrm{1D}}_{\mathrm{S,VD}} = \begin{pmatrix} H^{\mathrm{gg}} & 0\\ 0 & H^{\mathrm{ee}}\end{pmatrix}\ , \tag{S17}$$

respectively.

Hierarchical Equations of Motion. Here we assume that each chromophore is independently coupled to a heat bath. The correlation function of the collective bath operator can be written as:

$$\begin{aligned}C(t)=C_j(t) &= \frac{\mathrm{Tr_B}\left\{e^{-\beta H_B}e^{iH_B t/\hbar}\hat{B}_j e^{-iH_B t/\hbar}\hat{B}_j\right\}}{\mathrm{Tr_B}\left\{e^{-\beta H_B}\right\}}\\ &=\hbar\int_{-\infty}^{\infty}d\omega J(\omega)\frac{e^{-i\omega t}}{1-e^{-\beta\hbar\omega}}\ ,\end{aligned} \tag{S18}$$

where the spectral distribution function is given by $J(\omega)=J_j(\omega)=\sum_\xi\left[c^2_{j\xi}/2m_{j\xi}\omega_{j\xi}\right]\delta\left(\omega-\omega_{j\xi}\right)$. The phonon bath is modeled as a series of overdamped harmonic oscillators, and thus we employ the Drude spectral density $J(\omega)=2\lambda\gamma\omega/\pi(\omega^2+\gamma^2)$ to describe each phonon bath, where γ is the Drude decay constant and λ is the reorganization energy. In the current study we used $\hbar\gamma=125\ \mathrm{cm}^{-1}$ and $\lambda=150\ \mathrm{cm}^{-1}$, which are reasonable values for dye molecules in a methanol environment (1–3).

After applying the Drude spectral density, the correlation function becomes a sum of multiple exponential functions $C(t>0)=\sum_{k=0}^{\infty}c_k e^{-\nu_k t}$, where $\nu_0=\gamma$ and for $k\geqslant 1$, $\nu_k=2k\pi/\beta\hbar$ are known as the Matsubara frequencies. The constants, c_k, are given by:

$$\begin{aligned}c_0 &= \hbar\lambda\gamma\left[\cot\left(\frac{\beta\hbar\gamma}{2}\right)-i\right]\ ,\\ c_k &= \frac{4\lambda\gamma}{\beta}\frac{\nu_k}{\nu_k^2-\gamma^2}\quad ,\quad \text{for}\, k\geqslant 1\ .\end{aligned} \tag{S19}$$

We implemented the HEOM scheme developed by Shi *et al.*, which is a scaled version of HEOM that improves convergence with respect to the number of Matsubara frequencies included in the bath correlation function (4). The detailed form of the scaled HEOM reads as:

$$\begin{aligned}\frac{d}{dt}\tilde{\rho}_{\boldsymbol{n}} &= -\frac{i}{\hbar}\left[\hat{H}_{\mathrm{eff}},\ \tilde{\rho}_{\boldsymbol{n}}\right]-\left(\sum_{j=1}^{N}\sum_{k=0}^{K}n_{jk}\nu_k\right)\tilde{\rho}_{\boldsymbol{n}}\\ &-\frac{1}{\hbar^2}\sum_{k=K+1}^{\infty}\left(\frac{c_k}{\nu_k}\right)\sum_{j=1}^{N}\left[\hat{V}_j,\ \left[\hat{V}_j,\ \tilde{\rho}_{\boldsymbol{n}}\right]\right]\\ &-\frac{i}{\hbar}\sum_{j=1}^{N}\sum_{k=0}^{K}\sqrt{(n_{jk}+1)|c_k|}\left[\hat{V}_j,\ \tilde{\rho}_{\boldsymbol{n}^+_{\boldsymbol{jk}}}\right]\\ &-\frac{i}{\hbar}\sum_{j=1}^{N}\sum_{k=0}^{K}\sqrt{\frac{n_{jk}}{|c_k|}}\left(c_k\hat{V}_j\,\tilde{\rho}_{\boldsymbol{n}^-_{\boldsymbol{jk}}}-c^*_k\tilde{\rho}_{\boldsymbol{n}^-_{\boldsymbol{jk}}}\hat{V}_j\right)\ ,\end{aligned} \tag{S20}$$

with the Ishizaki-Tanimura truncating scheme $\nu_k e^{-\nu_k t}\simeq\delta(t)$ applied to the $k>K$ Matsubara frequencies (5, 6).

Within Eq. S20, $\boldsymbol{n}\equiv\{\boldsymbol{n}_1,\boldsymbol{n}_2,\cdots,\boldsymbol{n}_N\}=\{\{n_{10},n_{11},\cdots,n_{1K}\},\cdots,\{n_{N0},n_{N1},\cdots,n_{NK}\}\}$, where n_{jk} are non-negative integers. $\boldsymbol{n}^{\pm}_{\boldsymbol{jk}}$ refers to the change in value of n_{jk} to $n_{jk}\pm 1$ in the globally indexed site $\boldsymbol{n}$. The density operator with all zero indices is the system's reduced density operator (RDO), while all other operators are auxiliary density operators (ADOs). The hierarchical level of density operators is truncated to N_C; defined by $N_C=\max\sum_{j,k}n_{jk}$, which limits the total number of density operators to $C^{N_C+N}_{N_C}$. However, if one uses n_v vibrational

states for each chromophore, this will generate Nn_v^N single excited states and $N(N-1)n_v^N/2$ double excited states. Because the dimensions of the system Hamiltonian increase exponentially with n_v, we limit the total number of vibrational quanta in the system to $N_V = \max \sum_j i_j = 3$. The highest truncation level for the simulations is $N_C = 4$. In this study, one single exponential term $c_0 e^{-\gamma t}$ is enough to describe the bath correlation function, and therefore $K = 0$ is used.

Optical Response Functions. The effects of weak electromagnetic fields upon electric dipoles can be simulated by using optical response functions. These response functions describe how a weakly-perturbed system behavior deviates from the behavior of its equilibrium counterpart. The linear absorption spectra can be calculated by the dipole autocorrelation function, $\langle \hat{\mu}(t)\hat{\mu} \rangle$, that constitutes the first-order optical response function (7):

$$R^{(1)}(t) = \frac{i}{\hbar} \langle [\hat{\mu}(t), \hat{\mu}] \rangle \, , \qquad \text{[S21]}$$

where $\hat{\mu}(t) \equiv e^{i\hat{H}_{\rm tot}/\hbar} \hat{\mu} e^{-i\hat{H}_{\rm tot}t/\hbar}$ is the dipole operator within the Heisenberg picture, and $\langle \cdots \rangle \equiv {\rm Tr}\{\cdots \hat{\rho}_{eq}\}$. $\hat{\rho}_{eq}$ is the density operator of the total system at its thermal equilibrium. In the case of ED we assume the total system is initially in a factorized state $\hat{\rho}_{eq} = |0\rangle\langle 0| \otimes e^{-\beta \hat{H}_B}/{\rm Tr}_B\{e^{-\beta \hat{H}_B}\}$, where $\beta = 1/k_{\rm B}T$ is the inverse temperature. For VD, because of the possible thermal vibrational excitations, $\hat{\rho}_{eq}$ is obtained by equilibrating the total system with the initial factorized state using HEOM (Eq. S20).

In Eq. S21, the total dipole operator is defined by $\hat{\mu} = \hat{\mu}_+ + \hat{\mu}_- = \sum_j \mu_j (\hat{F}_j^\dagger + \hat{F}_j)$, where $\hat{\mu}_+ = \sum_j \mu_j \hat{F}_j^\dagger$ and $\hat{\mu}_- = \sum_j \mu_j \hat{F}_j$. The transition dipole moment of chromophore j is calculated by $\mu_j = \boldsymbol{d}_j \cdot \boldsymbol{l}$, where $\boldsymbol{d}_j$ is the transition dipole vector and $\boldsymbol{l}$ is the laser polarization vector, while the quantity $|\mu_j|^2$ is the oscillator strength. The dipole autocorrelation function can then be obtained by:

$$\langle \hat{\mu}(t)\hat{\mu} \rangle = {\rm Tr}_S\{\hat{\mu}\, {\rm Tr}_B[e^{-i\hat{H}_{\rm tot}t} \hat{\mu} \hat{\rho}_{eq} e^{i\hat{H}_{\rm tot}t}]\} \, , \qquad \text{[S22]}$$

where the term ${\rm Tr}_B[e^{-i\hat{H}_{\rm tot}t} \hat{\mu} \hat{\rho_{eq}} e^{i\hat{H}_{\rm tot}t}]$ is the RDO at time t with $\hat{\rho}_{\rm tot}(0) = \hat{\mu}\hat{\rho_{eq}}$ assigned as the initial density matrix for time evolution using HEOM approach. Once $\langle \hat{\mu}(t)\hat{\mu} \rangle$ is obtained, the linear absorption spectra, $I(\omega)$, can be calculated by:

$$I(\omega) \propto {\rm Im} \int_0^\infty dt \; e^{i\omega t} R^{(1)}(t) \, . \qquad \text{[S23]}$$

To account for random orientations of individual chromophores within the sample during the spectral measurements, the rotational average is considered. Instead of sampling over the whole unit sphere, the rotational average can be obtained by averaging over the signals from three orthogonal laser polarizations (8).

2D rephasing spectra are generated by sequential interaction of three broadband laser pulses (with wave vectors $\boldsymbol{k}_1$, $\boldsymbol{k}_2$, and $\boldsymbol{k}_3$) inside a sample to create a third-order polarization. The four-wave mixing field is then generated in the $\boldsymbol{k}_{\rm RP} = -\boldsymbol{k}_1 + \boldsymbol{k}_2 + \boldsymbol{k}_3$ direction and heterodyne-detected after superposing a fourth (local oscillator) $\boldsymbol{k}_4 = \boldsymbol{k}_{\rm RP}$ pulse. This generates a three-dimensional signal described by a third order nonlinear response function:

$$R^{(3)}_{\rm RP}(t_3, t_2, t_1) = -\frac{i}{\hbar^3} {\rm Tr}\left\{\hat{\mu}_- \hat{\mathcal{G}}(t_3) \hat{\mu}_+^\times \hat{\mathcal{G}}(t_2) \hat{\mu}_+^\times \hat{\mathcal{G}}(t_1) \hat{\mu}_-^\times \hat{\rho}_{eq}\right\} \, , \qquad \text{[S24]}$$

where $t_i (i = 1, 2, 3)$ are the time delays between sequential pulses $\boldsymbol{k}_i$ and $\boldsymbol{k}_{i+1}$ in the pulse sequence, and the superoperator notation $\hat{\mathcal{A}}^\times \hat{\mathcal{B}} = \hat{\mathcal{A}}\hat{\mathcal{B}} - \hat{\mathcal{B}}\hat{\mathcal{A}}$ is introduced for any operators. The evolution superoperator is defined through $\mathcal{G}(t)\rho = e^{-i\hat{H}_{\rm tot}t/\hbar} \rho e^{i\hat{H}_{\rm tot}t/\hbar}$, and the time evolution is calculated by the HEOM method. After a double Fourier transform on Eq. S24, the 2D rephasing spectra at waiting time t_2 is obtained by:

$$S^{(3)}_{\rm RP}(\omega_3, t_2, \omega_1) = {\rm Im} \int_0^\infty dt_1 e^{-i\omega_1 t_1} \int_0^\infty dt_3 e^{i\omega_3 t_3} \cdot R^{(3)}_{\rm RP}(t_3, t_2, t_1) \, . \qquad \text{[S25]}$$

The rotational average of the above equation is calculated by averaging the signal generated by ten laser polarization vectors aligning with the vertices of a dodecahedron in half of the coordinate space. It has been shown that the difference between the signal average generated through this method and the result obtained from 10^4 random polarization vectors provided by the Monte-Carlo method are within 1% (8).

Fourier Maps from Residual 2D Spectra . For the identification of the origins associated with oscillating spectroscopic features at specific beating frequencies, Fourier maps are generated by fitting all the t_2-evolving data points in the 2D spectra to exponentially decaying functions and subsequently performing a Fourier transform of the residual signal over t_2:

$$A(\omega_1, \omega_2, \omega_3) = \int_0^\infty dt_2 e^{-i\omega_2 t_2} S_{\rm res}(\omega_1, t_2, \omega_3) \, . \qquad \text{[S26]}$$

The technical details behind obtaining the residual spectra, $S_{\rm res}(\omega_1, t_2, \omega_3)$, are introduced in ref. (9). After generating the Fourier maps, the largest amplitude of the map at each specific ω_2 is collected through $A_{\max}(\omega_2) = \max |A(\omega_1, \omega_2, \omega_3)|$ to assist in characterization of important oscillation frequencies.

1. Halpin A, et al. (2014) Two-dimensional spectroscopy of a molecular dimer unveils the effects of vibronic coupling on exciton coherences. *Nat. Chem.* 6(3):196–201.
2. DeCamp MF, et al. (2005) Amide i vibrational dynamics of n-methylacetamide in polar solvents: The role of electrostatic interactions. *Journal of Physical Chemistry B* 109(21):11016–11026.
3. Jansen TL, Knoester J (2006) A transferable electrostatic map for solvation effects on amide i vibrations and its application to linear and two-dimensional spectroscopy. *Journal of Chemical Physics* 124(4):044502.
4. Shi Q, Chen LP, Nan GJ, Xu RX, Yan YJ (2009) Efficient hierarchical liouville space propagator to quantum dissipative dynamics. *J. Chem. Phys.* 130(8):084105.
5. Tanimura Y (2006) Stochastic liouville, langevin, fokker–planck, and master equation approaches to quantum dissipative systems. *J. Phys. Soc. Jpn.* 75:082001.
6. Ishizaki A, Tanimura Y (2005) Quantum dynamics of system strongly coupled to low-temperature colored noise bath: Reduced hierarchy equations approach. *J. Phys. Soc. Jpn.* 74(12):3131–3134.
7. Mukamel S (1995) *Principles of Nonlinear Optical Spectroscopy.* (Oxford University Press, New York).
8. Hein B, Kreisbeck C, Kramer T, Rodriguez M (2012) Modelling of oscillations in two-dimensional echo-spectra of the fenna-matthews-olson complex. *New Journal of Physics* 14:023018.
9. Milota F, et al. (2013) Vibronic and vibrational coherences in two-dimensional electronic spectra of supramolecular j-aggregates. *The Journal of Physical Chemistry A* 117(29):6007–6014.

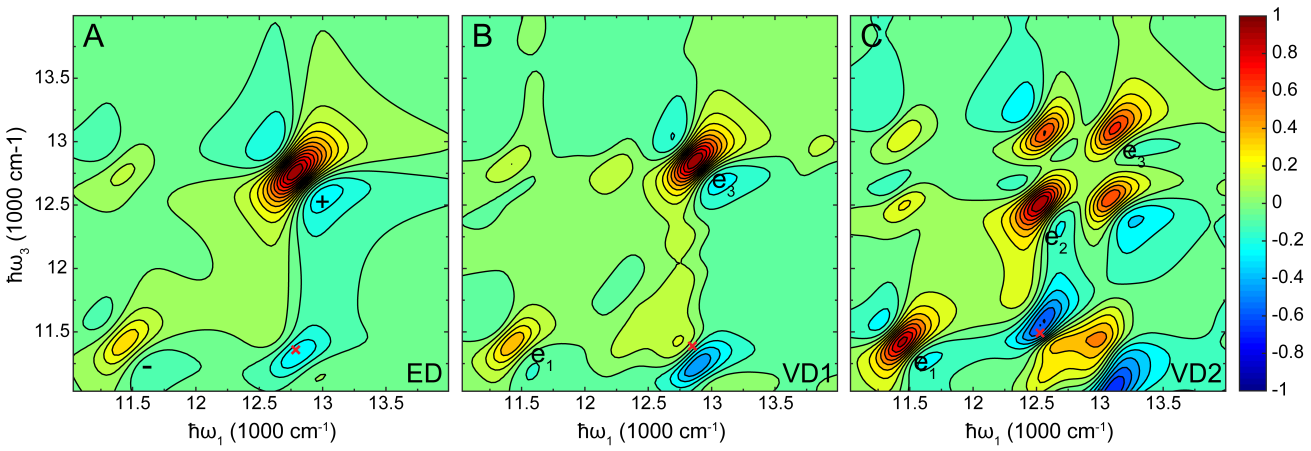

Fig. S1. The room-temperature rephasing 2DES at waiting time $t_2 = 0$ fs of ED (A), VD1 (B), and VD2 (C). The horizontal axis is the excitation energy $\hbar\omega_1$, and the vertical axis is the detection energy $\hbar\omega_3$. The eigenstates correspond to the diagonal peaks in the 2D spectra are labeled alongside. The normalized amplitude of the 2D spectra is indicated by color with evenly spaced contour lines. The crosses mark the cross-peaks CP_{+-} (A), CP_{31} (B), and CP_{21} (C), respectively.

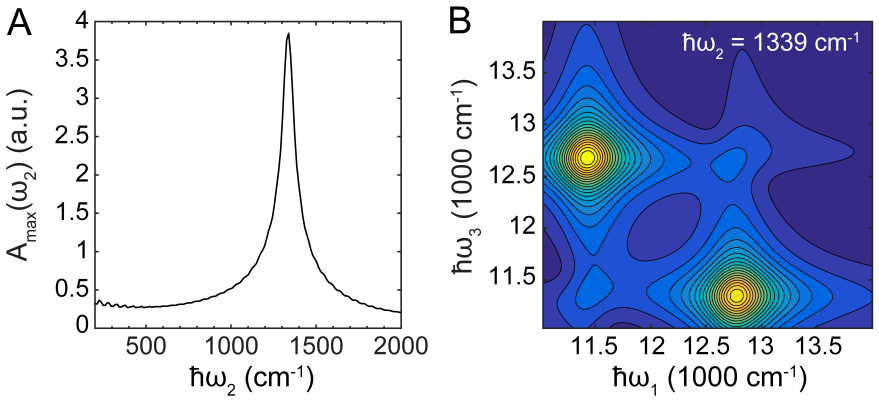

Fig. S2. Maximum of the Fourier map indicating t_2 oscillations in the 2DES of ED (A). Single oscillation frequency is found at 1339 cm^{-1}. The corresponding Fourier map is shown in (B).

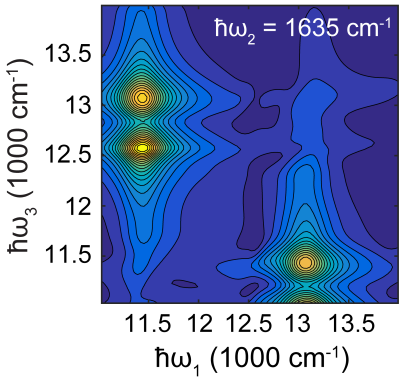

Fig. S3. The Fourier map of $\hbar\omega_2 = 1635$ cm^{-1} in VD2, shown for completeness with reference to Fig. 3 of the main text.

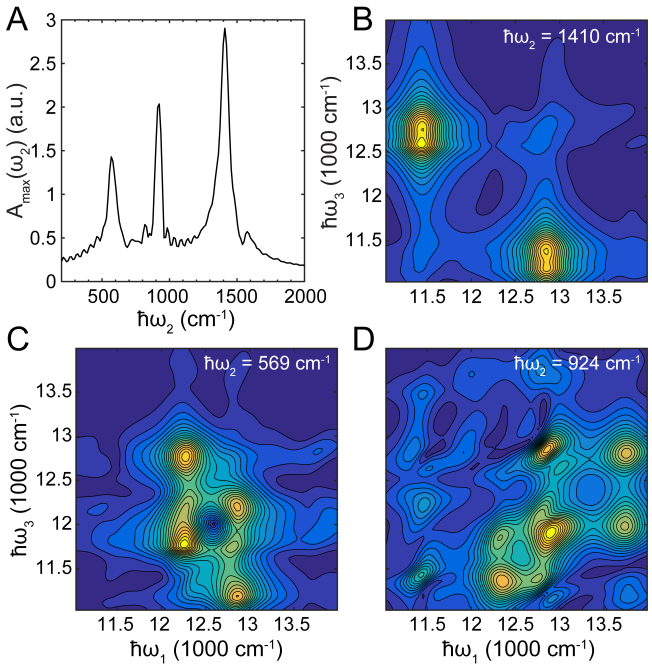

Fig. S4. Maximum of the Fourier map indicating t_2 oscillations in the 2DES of VD1 (A). Three major oscillation frequencies are found, from left to right they represent the e_2-e_3 transition, vibrational mode, and the e_1-e_3 transition, respectively. The corresponding Fourier maps are shown in subfigures (B), (C) and (D).

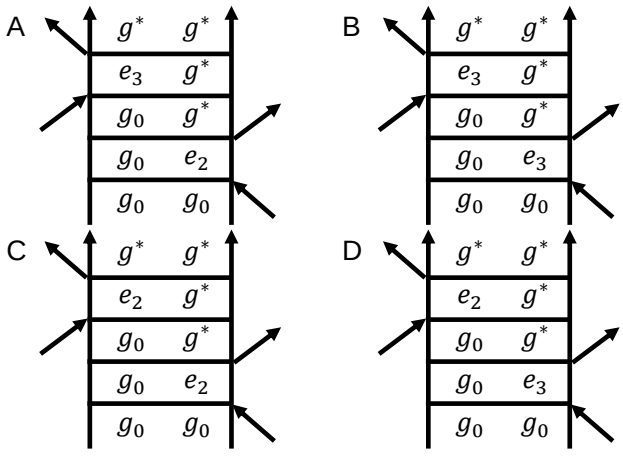

Fig. S5. The double sided Feynman diagrams for the ground state bleaching (GSB) contribution in the 2D rephasing spectra of VD2, only the major contributions are shown here, where subfigures (A), (B), (C) and (D) correspond to the features in Fig. 3D of the main text marked by square, triangle, circle, and cross, respectively. Here $g_0 \equiv g^{(0,0)}$ represents the vacuum state, and $g^* = g^{(0,1)}$ (or $g^{(1,0)}$) represents the one-phonon states in the zero-exciton manifold.

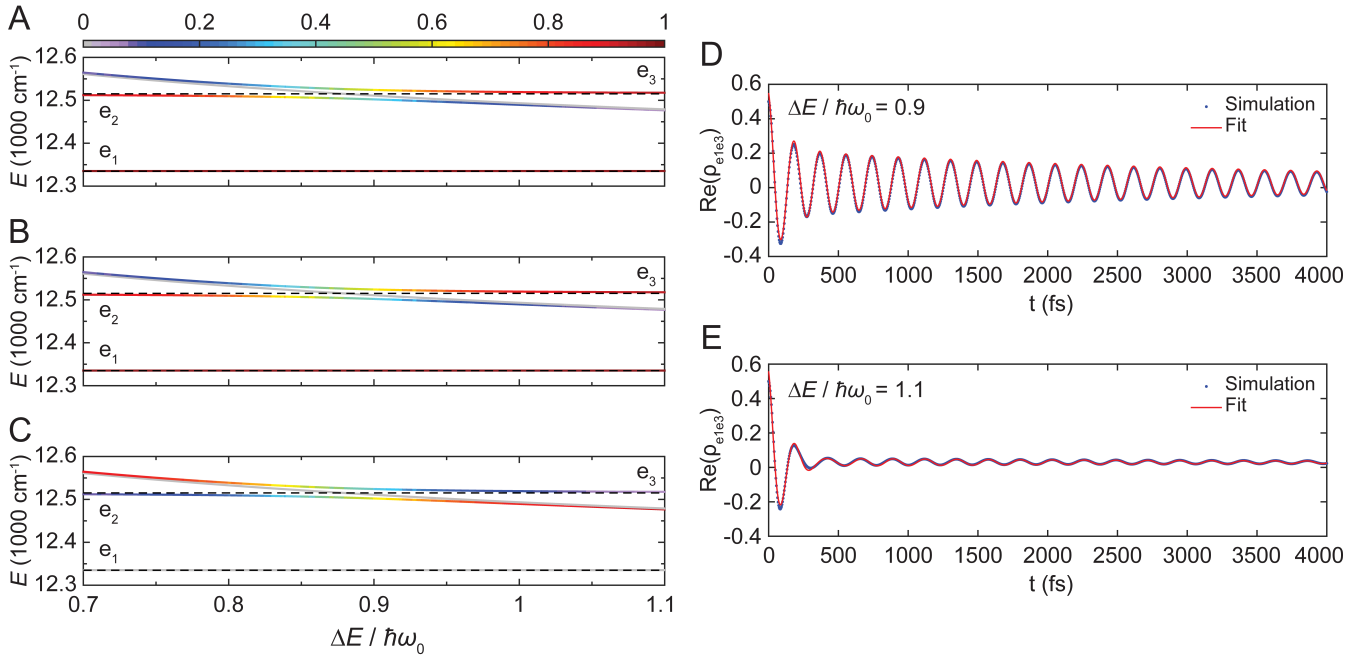

Fig. S6. For all the above subfigures, we examine a vibronic heterodimer model that features the bacteriochlorophylls 3 and 4 in the FMO complex of *Chlorobaculum tepidum*. In the left column, the four lowest eigenenergies in the one-exciton manifold with color representing oscillator strengths (**A**), electronic state character χ_{el} (**B**), and anticorrelated vibrational character χ_{v-} (**C**) are calculated with $E_1 = 12350$ cm^{-1}, $E_2 = 12500$ cm^{-1}, $J = -50$ cm^{-1}, $S = 0.025$, and the angle between the two transition dipoles are set to 90°. The energy gap $\Delta E = [(E_2 - E_1)^2 + 4J^2]^{1/2}$ is set to 180.28 cm^{-1}. The black dash lines indicate the excitonic energy gap. A similar character-mixing feature is identified comparing to the homodimer model discussed in the main text. In the right column, the coherence dynamics between states e_1 and e_3 at 77 K are shown under near-resonant (**D**) and off-resonant (**E**) conditions, using a superposition state $(|e_1\rangle + |e_3\rangle)/\sqrt{2}$ as an initial state. $\lambda = 35$ cm^{-1}, $(\eta_{\mathrm{E}}, \eta_{\mathrm{V}}) = (1, 0.25)$, and bath relaxation time γ^{-1} of 100 fs are used for the time evolution calculations. At off-resonant condition ($\Delta E/\hbar\omega_0 = 1.1$), the coherence lifetimes obtained from fitting to two exponentially decaying sinusoidal functions are $\tau_{21} = 3.29$ ps and $\tau_{31} = 106.8$ fs, with amplitudes of 0.026 and 0.508, respectively. Although possessing a small amplitude, the coherence between states e_1 and e_2 can be observed in the dynamics due to the phonon-induced energy relaxation from e_3 to e_2. At near-resonant condition ($\Delta E/\hbar\omega_0 = 0.9$), the lifetimes obtained are $\tau_{21} = 112.25$ fs and $\tau_{31} = 3.74$ ps, with amplitudes of 0.337 and 0.191, respectively. Under near-resonant conditions, the e_1-e_3 coherence lifetime is enhanced due to electronic-vibrational mixing and an amplitude increase of ps-long oscillation is observed. Additionally, the larger amplitude associated with the e_1-e_2 coherence suggests a faster energy relaxation. For reference, the vibrational coherence lifetimes at near- and off-resonant conditions are 6.86 ps and 5.71 ps, respectively.

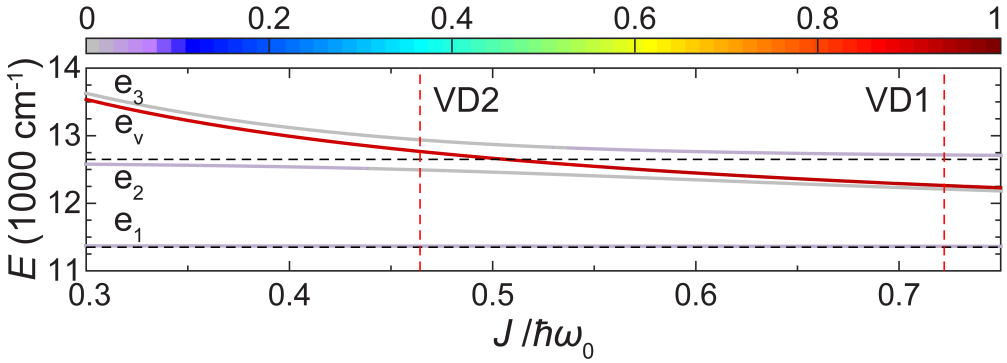

Fig. S7. Correlated vibrational contribution χ_{v+} (color) of the four lowest-energy eigenstates in the one-exciton manifold of VD. χ_{v+} is calculated as $\langle g^1_+|\mathrm{Tr}_{\mathrm{E}}\rho(t)|g^1_+\rangle$, where $\rho(t)$ is the system density matrix and $|g^1_+\rangle \equiv (|g^{(1,0)}\rangle + |g^{(0,1)}\rangle)/\sqrt{2}$ stands for the one-phonon state of the correlated vibrational mode. Almost all the correlated vibrational character is solely in state e_v, and thus this feature does not involve in the redistribution of oscillator strength by the mixing of electronic and vibrational degrees of freedom.